Formation of secondary aerosols from the ozonolysis of styrene: effect of SO_2 and H_2O.

Diaz-de-Mera, Yolanda[1]; Aranda, Alfonso[1]; Martínez, Ernesto[2]; Rodríguez, Ana Angustias[2]; Rodríguez, Diana[3]; Rodriguez, Ana[3].

[1]Universidad de Castilla-La Mancha. Facultad de Ciencias y Tecnologias Quimicas. Avenida Camilo José Cela s/n, 13071. Ciudad real. Spain.

[2] Universidad de Castilla-La Mancha. Instituto de Investigación en Combustión y Contaminación Atmosférica, Camino Moledores, s/n, 13071 – Ciudad Real. Spain.

[3]Universidad de Castilla-La Mancha. Facultad de Ciencias Ambientales y Bioquímica. Avenida Carlos III s/n, 45071 Toledo, Spain.

Correspondence to: Alfonso Aranda (alfonso.aranda@uclm.es)

Abstract. In this work we report the study of the ozonolysis of styrene and the reaction conditions leading to the formation of secondary aerosols. The reactions have been carried out in a Teflon chamber filled with synthetic air mixtures at atmospheric pressure and room temperature. We have found that the ozonolysis of styrene in the presence of low concentrations of SO_2 readily produces new particles under concentrations of reactants lower than those required in experiments in the absence of SO_2. Thus, nucleation events occur at concentrations around $(5.6\pm1.7)x10^{8}$molecule cm^{-3} (errors are $2\sigma\pm20\%$) and SO_2 is consumed during the experiments. The reaction of the Criegee intermediates with SO_2 to produce SO_3 and then H_2SO_4 may explain (together with OH reactions' contribution) the high capacity of styrene to produce particulate matter in polluted atmospheres.

The formation of secondary aerosols in the smog chamber is inhibited under high H_2O concentrations. So, the potential formation of secondary aerosols under atmospheric conditions depends on the concentration of SO_2 and relative humidity, with a water to SO_2 rate constants ratio $k_{H2O}/k_{SO2}= (2.8\pm0.7)\times10^{-5}$ (errors are $2\sigma\pm20\%$).

1. Introduction.

Styrene is one of the most important monomers worldwide. The double bond in the vinyl group enables polymerisation and so the production of widespread used materials such as polystyrene, styrene–butadiene rubber, styrene–butadiene latex, etc. Despite the high reactivity of styrene in the atmosphere, it can be considered as an ubiquitous species due to the wide range of different

anthropogenic sources. Thus, it has been measured in remote areas (Kos et al., 2014), in indoor air samples (Sarigiannis et al., 2011; Xu et al., 2016), or in ambient air (Kabir and Kim, 2010; Li et al., 2014).

Styrene is naturally produced as a degradation product in cinnamic acid containing plants (Duke, 1985) and as a by-product of fungi and microbe metabolism (Shimada et al., 1992). Nevertheless, the presence of styrene in the atmosphere is mainly due to fugitive emissions from petrochemical facilities and industrial processes involving styrene or its polymers (Knighton et al., 2012; Zhang et al., 2017). Other sources include the release from styrene-based materials, incineration of styrene polymers, or cigarette smoke for indoor air. The combustion of traditional petroleum-based fuels or the alternative newly developed biofuels are also responsible of important exhaust emissions of styrene mainly in populated areas (Lopes et al., 2014; Li et al., 2015; Hu et al., 2017).

Styrene is a hazardous air pollutant and so its emissions are regulated by the environmental protection agencies (EPA, 2017). The exposure to inhalation or intake of styrene through food or drinks may lead to severe health effects (ATSDR, 2017).

The main gas phase reactions of styrene in the atmosphere have been studied previously, being the reported room-temperature kinetic rate constants with OH, NO_3 and ozone (in cm^3 $molecule^{-1}$ s^{-1}): $5.8x10^{-11}$, $1.51x10^{-13}$ (Atkinson and Aschmann, 1988) and $1.5x10^{-17}$ (Le Person et al., 2008), respectively. The results obtained by Le Person et al. (Le Person et al., 2008) show that reactions with OH, NO_3 and O_3 are all important atmospheric loss processes for styrene in the gas phase.

On the other hand, photolysis of styrene constitutes a slower sink during daylight hours.

Recently, exposure to particulate matter is being associated to the decrease of life expectancy and numerous diseases, especially cardiopulmonary illness (Bates et al., 2015). The size of particles is a key factor for health effects since the potential ability to access the lungs becomes higher for the smaller ultrafine particles (Nel, 2005). This is a problem in urban air where particles with size diameter below 100 nm may account for 80–90 % of the total particle number concentration (Mejía et al., 2008). Apart from direct primary sources like vehicle exhausts, one of the main sources of ultrafine particles is the formation of secondary organic aerosols (SOA) from the reactions of the emissions of gas-phase pollutants (Cheung et al., 2013). In this sense, it has been found that aromatic compounds readily yield SOA under urban air conditions (Ng et al., 2007). The contribution of aromatic compounds to the total SOA formation may account from 78.5 to 91.9 %, well above those of alkanes and alkenes (Sun et al., 2016). Thus, given their high SOA formation potential, new approaches to predict the amount of aerosol formed from the oxidation of aromatic hydrocarbons are being developed (Li et al., 2016). In the case of styrene, it was identified as the second most efficient species forming SOA (15%), only after toluene (16%) (Sun et al., 2016).

For styrene, a theoretical model shows that its reaction with OH could contribute to the formation of SOA in polluted atmospheres (Wang et al., 2015). Furthermore, a previous experimental work has also reported the formation of SOA from the reaction of styrene with ozone and the effect of the presence of ammonia and water (Na et al., 2006).

Being styrene an alkene, its reaction with ozone proceeds through the formation of a Criegee intermediate (CI). Very recently, it has been found that stabilised CI (sCI) can undergo reactions with SO_2 several orders of magnitude faster than assumed so far (Welz et al., 2012) producing SO_3, which contributes efficiently to the formation of ground level sulfuric acid (Mauldin et al., 2012; Newland et al., 2015). Likewise, mixing SO_2 with gasoline vehicle exhausts has been shown to increase the formation of secondary aerosols (Liu et al. 2016). Thus, the reaction with SO_2 could be the key to explain the high SOA formation potential of styrene under polluted conditions. On the other hand, the competition of SO_2 and water vapour in the removal of sCI in the atmosphere depends on the CI structure (Berndt et al., 2014a; Díaz-de-Mera et al., 2017) and may play an important effect on the net SOA formation of this aromatic compound.

In this work we study the ozonolysis reaction of styrene following the conditions that lead to the formation and growth of new particles. The effect of water vapour and SO_2 concentrations during the process are also studied and discussed.

2. Experimental.

The experimental system consisted on a collapsible 200L Teflon reactor coupled to different detectors to analyse both the gas phase and particulate matter. The reactants' samples, styrene, cyclohexane and SO_2, were prepared in a volume-calibrated glass bulb with 100 and 1000Torr full scale capacitance pressure gauges, MKS 626AX, and then flushed to the reactor using synthetic air. Concentrations for each species were obtained from their partial pressures in the glass bulb and the final volume of the Teflon reactor.

The ozone was generated in-situ by passing pure oxygen through a high voltage electric discharge, BMT Messtechnik 802N, and then fed to the sampling bulb and to an absorption 10 cm long quartz cell to measure the concentration using a UV-vis Hamamatsu spectrometer, C10082CAH at 255nm. Once the concentration in the cell and bulb were known, it was diluted with synthetic air to get the required concentration in the reactor.

Cyclohexane in excess was used as OH radical scavenger in concentration ratios so that >97% of OH formed in the reactions was removed (Ma et al., 2009).

Water vapour in the reactor was introduced by passing the air flows carrying the reactants through a glass bubbler containing the calculated amount of water required for any given relative humidity

(RH). The sampled water was then evaporated and flushed inside the reactor through the flow of synthetic air. For the series of experiments carried out under "dry conditions" the synthetic air was used directly from the cylinder, with a water mixing ratio below 2ppm, which is the concentration stated by the supplier.

Typically, the reactants were sequentially introduced as follows: first, styrene, second cyclohexane (OH scavenger), then SO_2 and finally ozone. During the injection of ozone, the reactor was shaken to improve mixing and then the valves to the sampling detectors were open. Liquid water (when necessary) was introduced in the bubbler at the beginning, being flushed by the air carrying the rest of gaseous reactants.

The concentration of particles was monitored by an scanning mobility particle sizer (SMPS), TSI SMPS 3938 with a CPC particle counting 3775 and a nano-differential mobility analyser which improves size resolution over the particle size range 4.0-150nm. The SMPS was operated with 3.0 L min^{-1} sheath flow and 0.3 L min^{-1} sampling flow rate. Size distributions were recorded at 1 minute intervals from the injection of ozone and the total aerosol mass concentration was derived from the measured particle size distribution assuming unit density and spherical particles. Prior to each experiment the Teflon bag was repetitively washed with clean synthetic air until the level of particles was below 1 cm^{-3}.

SO_2 concentrations were measured by a fluorescence SO_2 analyser, Teledyne Instruments 101-E. Previous runs with only SO_2/air samples in the reactor showed that SO_2 wall losses were negligible. Additionally, no interference in the SO_2 fluorescence signal from the rest of co-reactants was observed in the range of concentrations used in this study.

Ozone concentrations were measured with an ozone analyser, Environment O342M. Several tests showed that O_3 losses in the reactor were negligible within the time scale of the experiments. Styrene also shows UV absorption at 255nm. Thus, several samples of styrene in air were introduced in the reactor to calibrate the O_3 analyzer for the styrene measurements. After a few minutes an important decrease in the styrene signal was observed (attributed to polymerisation within the UV detection cell) what prevents from monitoring the styrene temporal profiles in the reactor continuously. Nevertheless, when sampling of styrene was carried out intermittently for short time periods (and letting the UV absorption cell to completely evacuate the previous sample) the signal always recovered its initial intensity. Under dark conditions with different styrene concentrations in the reactor, no measurable consumption of styrene was observed from the periodic samples measured in the UV spectrometer for 80 minutes runs.

Reagents.

All the substances used were of the highest commercially available purity. Liquid reagents were purified by successive trap to trap distillation. Styrene >99%, Sigma-Aldrich; SO_2 99,9%, Fluka; cyclohexane 99.5%, Sigma-Aldrich; synthetic air 3X, Praxair; O_2 4X, Praxair.

3. Results and discussion.

3.1. Nucleation conditions.

For asymmetric alkenes like styrene, the ozonolylis leads to the formation of two different Criegee intermediates and the corresponding aldehydes: $C_6H_5C{\cdot}HOO{\cdot}$ and HCHO or $\cdot CH_2OO\cdot$ and C_6H_5CHO. For the title reaction, previous results show that the two pathways (leading to formaldehyde or benzaldehyde) are quantitative and with yields around 40 % (Tuazon et al., 1993). The subsequent reactions of the primary products, especially the Criegee intermediates (Na et al., 2006, Bernd et al., 2014a), may lead to the formation of secondary aerosols.

In order to approach real ambient air conditions, a series of experiments were carried out with ozone and styrene using concentrations lower than those of the study by Na et al., 2006. Thus for example, for initial styrene and ozone concentrations in the range of 10 ppbs, no particles were observed in the reactor after 60 minutes runs. The concentrations were then progressively increased and, for example, for experiments with concentrations of 100 ppb of styrene and 200 ppb of ozone, particles generated after 15 minutes. Since the gas-phase reaction of styrene with ozone has been reported previously with $k_{295K}=(1.5\pm0.3)x10^{-17} cm^3\,molecule^{-1}\,s^{-1}$ (Le Person et al., 2008), this kinetic rate constant can been used to simulate the ozone and styrene concentrations profiles. Thus, from the previous experiments, for 15 minutes reaction time the results show that the concentration of reacted styrene required for the formation of new particles is very high, $(1.6\pm0.5)x10^{11}$ molecule cm^{-3} (errors are $2\sigma\pm20\%$) and so the reaction of styrene with ozone is unlikely, by itself, to drive nucleation events under usual atmospheric conditions.

On the other hand, when carrying the experiments in the presence of SO_2, particles were generated at lower concentrations of reactants. Figure 1 shows the typical experimental profiles of the particle number concentration (PNbC), particle mass concentration (PMC) and the simulated profiles for styrene concentration and total reacted styrene. As we can see, after the initial time required to complete nucleation, the PMC increases linearly. Likewise, since the ozone and styrene reaction is slow, the reactant concentrations remain essentially constant and the reacted styrene increases linearly, like PMC. This behaviour suggests that the initial reaction is the rate limiting step in the formation of condensed matter under these experimental conditions.

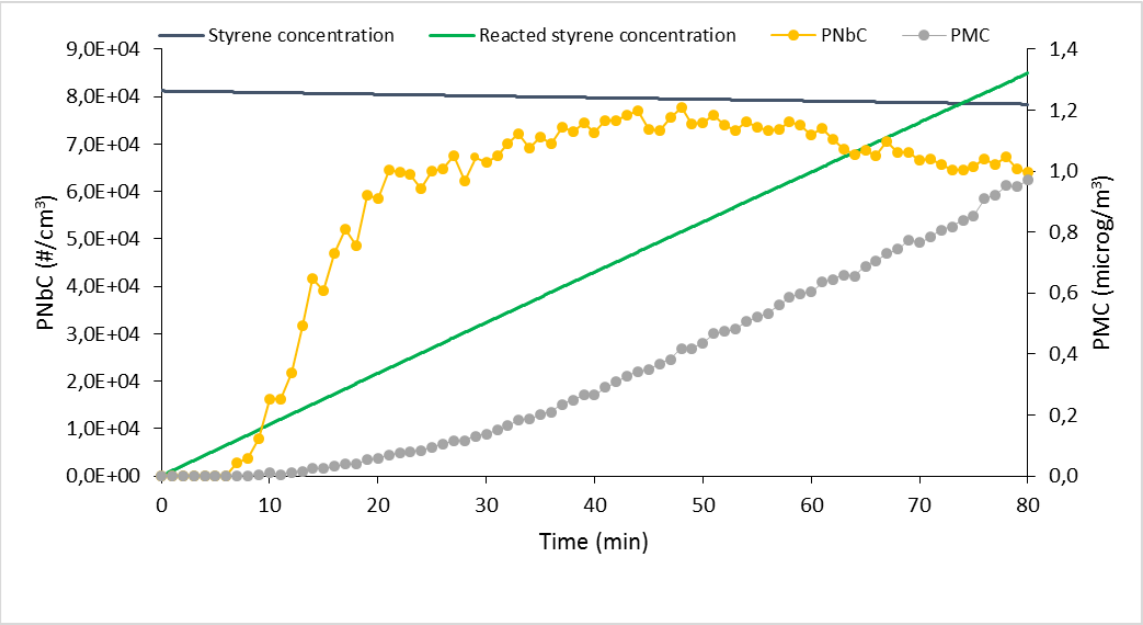

Figure 1. Experimental temporal profiles for particles (PNbC and PMC) and simulated profiles of styrene and reacted styrene. Initial concentrations: styrene, 10ppb; O_3, 20ppb and SO_2, 10ppb. RH=0%. Styrene and reacted styrene concentrations are shown multiplied by the required factors to display them in the same figure.

A series of experiments was conducted to measure the reacted concentration of styrene required for the generation of particles in the presence of SO_2. Thus, Figure 2 shows the concentrations of reacted styrene calculated at the nucleation events (assumed as the first scan with PNbC above 100 cm^{-3}) for experiments with SO_2 initial concentrations in the range 5-100 ppbs and fixed initial concentrations of styrene (10 ppb) and ozone (20 ppb). The burst of particles takes place at approximately the same reaction time and concentration of reacted styrene. So, increasing SO_2 concentration doesn't result into further acceleration of the nucleation event, which is found to occur once the reacted styrene amounts $(5.6\pm1.7)\times10^{8}$ molecule cm^{-3} (errors are $2\sigma\pm20\%$). This value is three orders of magnitude lower than in the absence of sulphur dioxide, showing that the SO_2 reactivity must play a key role in the nucleation steps. As shown above, lowering the concentrations of SO_2 rises the nucleation threshold (as inferred from the 5 ppb SO_2 experiment) up to 1.6×10^{11} molecule cm^{-3} for SO_2 zero concentration.

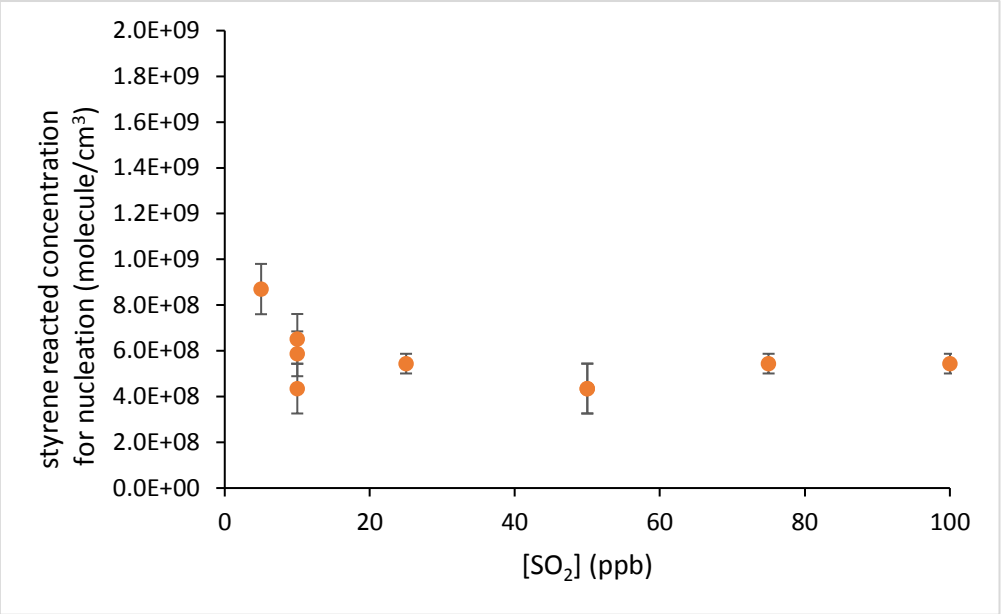

Figure 2. Concentration of reacted styrene at the instant of particles' appearance for experiments with different initial SO_2 concentrations. For this series of experiments, [styrene]=10ppb and [O_3]=20ppb. The displayed errors are σ.

3.2. Effect of styrene and ozone initial concentrations.

A series of experiments was carried out to assess the effect of styrene concentration on the formation of secondary aerosols. Figure 3 shows the results for PNbC, PMC and the mean particle size diameter for different [styrene]. The particles grew larger for higher concentrations of styrene with average diameters up to 45 nm and the number concentration of new particles rose up to $4x10^5$ cm^{-3} for experiments carried out under 10 ppb and 20 ppb initial concentrations of SO_2 and ozone respectively.

To assess the conversion of gas-phase reactants into aerosols we can use the fractional aerosol yield (Y) which may be defined (Odum et al., 1996) as the fraction of the reagent (styrene for this work), that is converted to aerosol:

$$Y = \frac{PMC}{\Delta C_8H_8}$$

Where PMC is the aerosol mass concentration (μg m^{-3}) produced for a given amount of reacted styrene, ΔC_8H_8 (in μg m^{-3}).

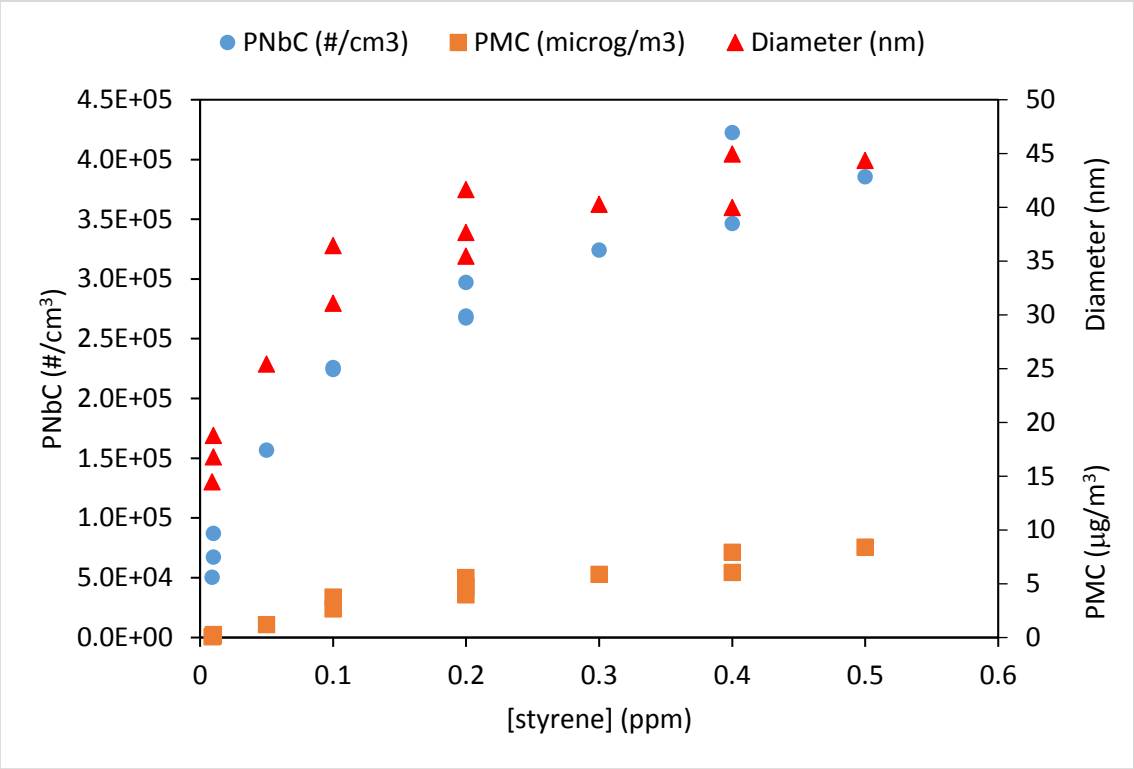

Figure 3. Particle mass concentration and mean particle size diameter versus styrene concentration at reaction time=40 min for 10 ppb and 20 ppb initial concentrations of SO_2 and ozone respectively. The maximum particle number concentration (PNbC) measured for each experiment are also plotted.

According to Odum's model, the growth of the aerosol's mass may be described as a gas-particle partitioning absorption mechanism where organic products may partition a portion of their mass at concentrations below their saturation concentration.

Figure 4 displays the particle mass concentration growth curves for several experiments with different initial styrene concentrations. After the first few minutes, once nucleation has occurred, the system exhibits nearly constant yields for the rest of the experiment. Furthermore, the yields from the different experiments are very similar.

The linearity of the fractional yield suggests that the aerosol mass comes quantitatively from a single product with very low volatility. This behaviour has been found also for the formation of SOA from other aromatic compounds such as benzene, m-xylene or toluene (Ng et al., 2007).

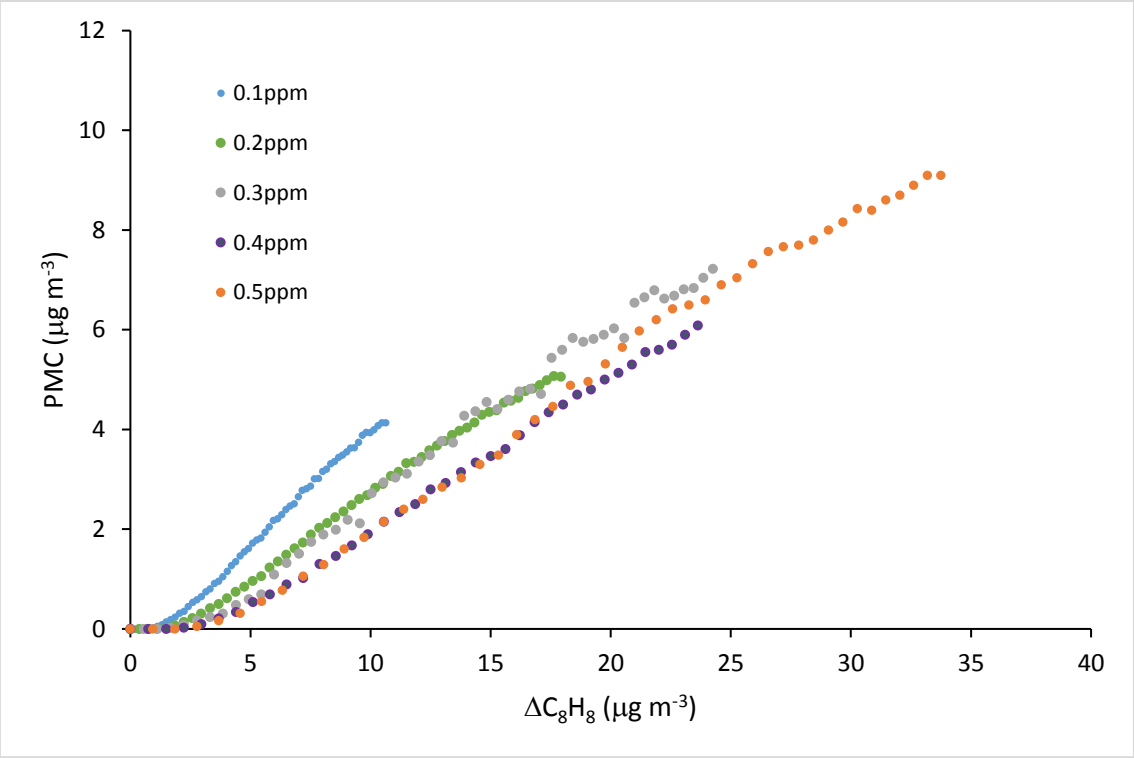

Figure 4. Particle mass concentration growth curves versus the reacted styrene for different initial styrene concentrations (see the legend). Fixed initial concentrations of sulphur dioxide and ozone were used: [SO2]=10 ppb and [O3]=20 ppb.

Figure S1 shows the yields obtained from the slopes of the linear fittings (straight part after the first few minutes) of the plot PMC versus ΔC_8H_8 (Figure 4) versus the styrene initial concentration affording an average fractional aerosol yield of 0.39±0.10 (errors are 2σ±20%). The dependence of the aerosol fractional yield on the initial concentration of styrene is weak as it is found in the plot. Nevertheless, for low styrene concentrations the yield values are slightly higher.

The effect of increasing ozone concentrations has been also studied in this work. A series of experiments fixing the initial concentrations of styrene and SO_2 was carried out with different initial concentrations of ozone in the range 10 ppb to 0.6 ppm. The increase of ozone led to the increase of PNbC, PMC and average particle size diameters, with a behaviour similar to the series changing styrene concentration described previously. The results are found in the supplementary material, Figures S2-S4.

3.3. Effect of SO_2 initial concentration.

As shown previously, the presence of SO_2 enhances the production of secondary aerosols from the ozonolysis reaction of styrene in air. To find the effect of SO_2 concentration in the mechanism,

different experiments were performed fixing the initial concentrations of styrene and ozone while the initial concentration of SO_2 was changed within the range 5 to 100 ppb. Even though the reacted styrene profile must be the same for all these experiments (since the same initial concentrations of O_3 and styrene are used), a significant increase in PNbC and PMC was observed for increasing SO_2 concentrations (mainly in the range 0-25 ppb), Figure 5. For $[SO_2]$ above approximately 25 ppb, further increases of SO_2 didn´t result in significant changes in the aerosol production. The calculated fractional aerosol yield also increased up with $[SO_2]$ to values around 2, as it is shown in Figure S5. From the definition of the fractional yield, values above unity are consistent since styrene is not the only species involved in the formation of secondary aerosol and so the mass of the particulate matter can be larger than the mass of the reacted styrene.

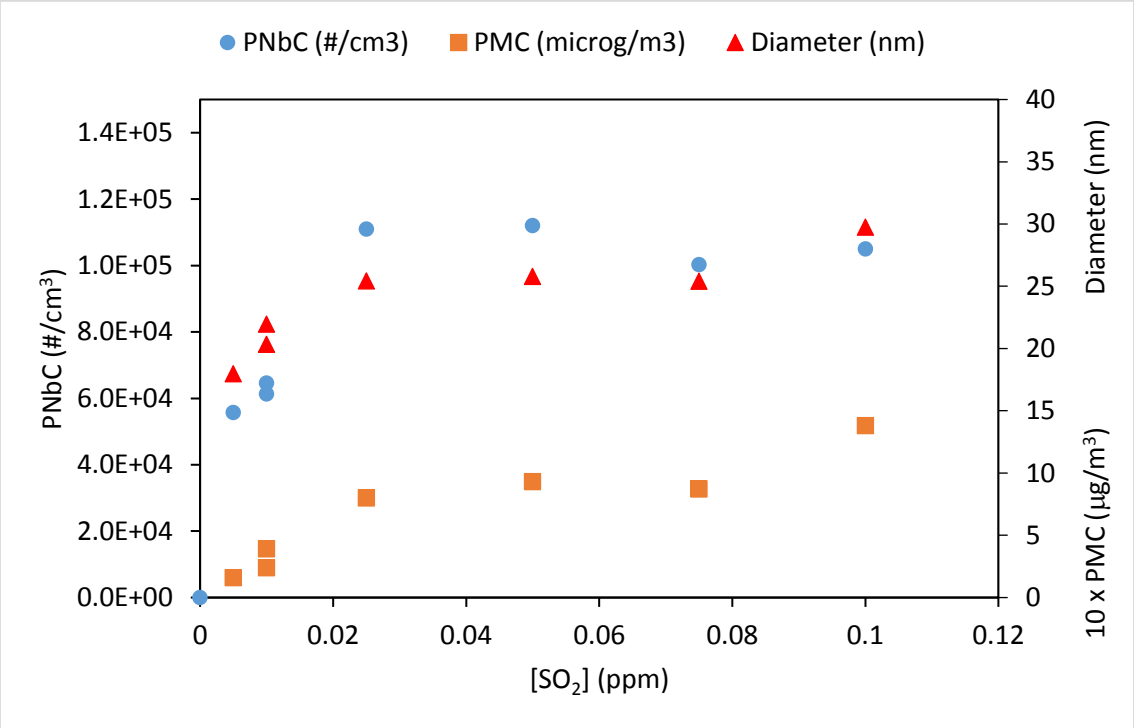

Figure 5: Effect of SO_2 concentration on the production of secondary aerosols. The maximum particle number concentration (PNbC) measured for each experiment are shown in the main axis. PMC and mean particle size diameter versus SO_2 concentration are shown at a fixed reaction time, 50 min (secondary axis), for 10 ppb and 20 ppb initial concentrations of styrene and ozone respectively.

SO_2 doesn't react with the initial reactants, cyclohexane, styrene or ozone within the time scale of the experiments nor with the aldehydes HCHO, C_6H_5CHO coming from the ozonolysis reaction. On the other hand, it is known that Criegee intermediates do undergo fast reactions with

SO_2 (Taatjes et al., 2013). Nevertheless, since the styrene-ozone reaction is slow, under the experimental conditions, Figure 5, the production rate of the Criegee intermediates is very low and a slight consumption of SO_2 was expected. Consistently, the experimental SO_2 temporal profiles during most of the experiments were nearly constant. Thus, in some experiments, to magnify the SO_2 consumption and make it measurable, it was necessary to increase the styrene and ozone concentrations (up to 100-200 ppb) while keeping [SO_2] in lower levels (around 20 ppb). For this series of experiments, the production of sCI was relatively high and the SO_2 concentration was observed to decrease with time (experimental SO_2 decays, Figure 6), which confirms that SO_2 reacts with the products from the ozonolysis.

Previous studies have shown that the first step of the reaction of sCI (R^1R^2COO) with SO_2 is the formation of a cyclic secondary ozonide which can undergo isomerisation (only possible if R^2 is an H-atom), leading to an organic acid (R^1COOH) and SO_2, or decomposition to a carbonyl compound (R^1R^2CO) and SO_3 (Jiang et al.,2010; Kurten et al., 2011). The organic acids will generally be less volatile than their alkene precursors and SO_3 readily produces H_2SO_4 in the presence of water vapour. Such products are expected to be involved in the formation and growth of new particles.

In the isomerisation channel, SO_2 would behave as a catalyst in the production of acids (Díaz de Mera et al., 2017). On the other hand, in this work we have found, Figure 6, that there is a net consumption of SO_2 and that the amount of reacted SO_2 increases with the reaction time coordinate. This fact suggests that for the case of styrene ozonolysis the reaction of the sCI with SO_2 proceeds at least in part through the oxidation channel leading to SO_3.

Some of the previous experiments were carried out under the presence of water under different RH. For example, as shown in Figure 6, when water vapour is present (RH=5 % in the plotted experiment) the decrease in SO_2 was significantly lower than under drier conditions. These results suggest that H_2O and SO_2 constitute competitive sinks for the stabilised Criegee intermediates.

For these experiments we assume a simple mechanism as follows:

Styrene + O_3 → HCHO + C6H5CHO + CI + sCI (1)

sCI + SO_2 → intermediates (SO_3) → secondary aerosols (2)

sCI+ H_2O → P3 (3)

Where sCI includes both $\cdot CH_2OO\cdot$ and $C_6H_5C\cdot HOO\cdot$ (Tuazon et al., 1993), the latter being possible as conformer syn or anti. (Vereecken and Francisco, 2012).

For the case of $\cdot CH_2OO\cdot$, the reaction with SO_2 has been studied previously and the available experimental data show that it leads to the formation of SO_3 with a unity yield (Berndt et al., 2014a; Berndt et al., 2014b). In this study, for the experiments carried out in the drier conditions

(RH close to zero), the water concentration ratio is in the order of 2ppm ($5x10^{13}$ molecule cm^{-3}). The H_2O-SO_3 gas-phase reaction is very fast, $k= 3.90x10^{-41}exp(6830.6/T)[H2O]^2$ (Jayne et al., 1997) and the gas-phase water concentration is high enough to react with SO_3, leading to H_2SO_4 (Díaz-de-Mera et al., 2017), which is the species assumed to generate new particles in the system.

For the other sCI formed from the styrene ozonolysys, $C_6H_5C{\cdot}HOO{\cdot}$, the oxidation channel leading to SO_3, and then H_2SO_4, is also possible and can contribute to the nucleation step. Recent works have shown that the oxidation channel also generates H_2SO_4 quantitatively in the ozonolysis of other alkenes such as trans-2-butene and 2,3-dimethyl-2-butene when it happens in the presence of SO_2 (Bernd et al., 2014a). Furthermore, the crossed reaction between the biradical $C_6H_5C{\cdot}HOO{\cdot}$ and formaldehyde has been suggested to produce 3,5-diphenyl-1,2,4-trioxolane (Na et al., 2006) and the secondary ozonide may also undergo partial conversion into a hydroxyl-substituted ester (Tuazon et al., 1993). These low volatile products may contribute to the growing of particles.

In this work we have studied the direct yield for the reaction between sCI and SO_2. As shown previously, the correlation between the measured MPC and the reacted styrene points out the ozonolysis as the rate limiting step for SOA production. Thus, the sCI/SO_2 reaction is expected to be much faster than the styrene/ozone reaction and, so, the amount of consumed SO_2 should correlate with the total reacted styrene. In this sense, Figure 6 shows the results for several experiments with different initial concentrations of styrene and ozone under dry conditions. The simulated profiles for total reacted styrene are nearly straight lines since its precursors, styrene and ozone remain essentially constant during the experiment. The total reacted SO_2, measured experimentally, also shows linear temporal profiles except for the experiments with the higher concentrations of styrene and ozone. From the ratio of the slopes of the linear fits (reacted SO_2 and reacted styrene) we derived an average yield for reaction (2) with respect to the initial reaction (1), Table 1, $\eta= 0.51\pm0.13$ (errors are $2\sigma\pm20\%$).

For the experiments with higher concentrations, for example 200 ppb of both styrene and ozone, the SO_2 concentration dropped from 20 to 10 ppb after 25 minutes lowering the rate of the sCI/SO_2 reaction and driving to the curvature of the temporal profile of the reacted SO_2. For such experiments the yield for reaction (2) was obtained from the initial data (20 min in the shown experiment) where the SO_2 data can still be fitted to a straight line.

The measurement of the yield for reaction 2 could not be carried out within a wide range of [SO_2] initial concentrations since the ozonolysis reaction is slow and increasing SO_2 leads to very small changes in the SO_2 signal.

The results show that sCI react quantitatively through reaction (2) in the presence of SO_2 with a constant yield regardless the initial concentrations of styrene and ozone. However, as sCI can

react through different competitive sinks, it is expected that the yield of reaction (2) depends on the concentration of SO_2, water and other possibly involved species.

Table 1. Yield of reaction (2) (consumption of SO_2) after the ozonolysis of styrene (reaction 1). The yields are obtained from the ratio of the reacted SO_2, and the reacted styrene. Errors are 2σ.

[Styrene]/ppb	[O_3] /ppb	[SO_2] /ppb	RH	η
200	100	20	0%	0.47± 0.05
100	200	20	0%	0.55±0.06
100	100	20	0%	0.54±0.05
200	200	20	0%	0.48±0.06

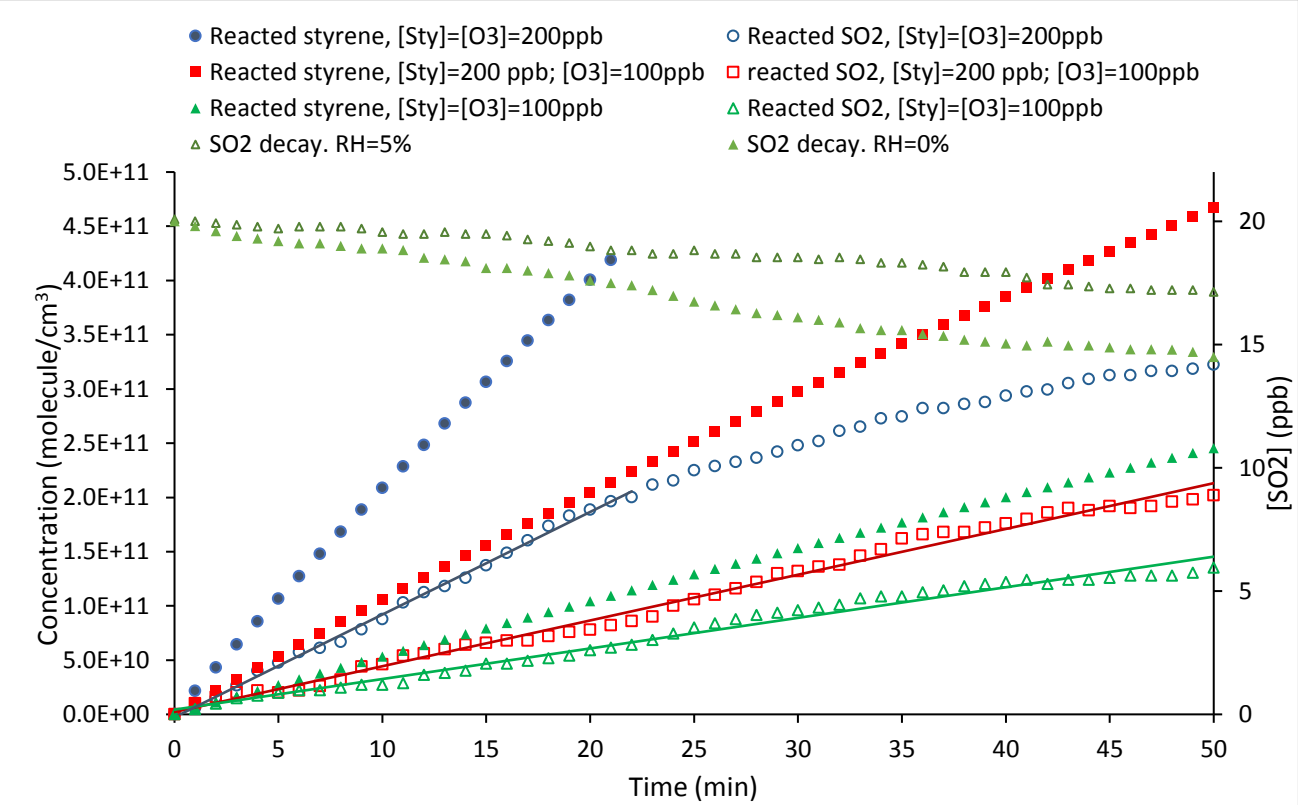

Figure 6. SO_2 experimental decays for 100 ppb of styrene and ozone (initial concentrations) under dry conditions and with RH=5 %. Simulated profiles for total reacted styrene under different initial concentrations of styrene and ozone (see the legend) and the corresponding experimental profiles for total reacted SO_2. The initial SO_2 concentration was 20 ppb for all the experiments displayed.

3.4. Effect of water vapour.

A series of experiments with concentrations or reactants around 10 ppb was carried out to study the effect of RH on the production of SOA. For these experiments the PMC values were very small, always below 0.5 μg m^{-3} and the concentrations had to be increased to get more accurate mass data. Figures 7 and S6-S8 show the results for PNC, PMC and average particles' size diameters for experiments with 20 ppb of styrene and SO_2, 40 ppb of ozone and RH in the range 0-35 %.

As it is found in Figure 7, the addition of water, induces a significant drop (mainly in the RH range below 10 %) on the PNbC and inhibits their growing leading to lower production of SOA. These results are consistent with the suggested mechanism where SO_2 and H_2O compete to scavenge the Criegee intermediates (reactions (2) and (3)). The reaction with water vapour is expected to proceed through the addition of the water oxygen atom to the carbon atom in the carbonyl oxide and the simultaneous transfer of one hydrogen atom from the water molecule to the terminal O atom in the CI (Anglada et al., 2011), leading to α-hydroxi-hydroperoxides that can subsequently decompose or react with other atmospheric species.

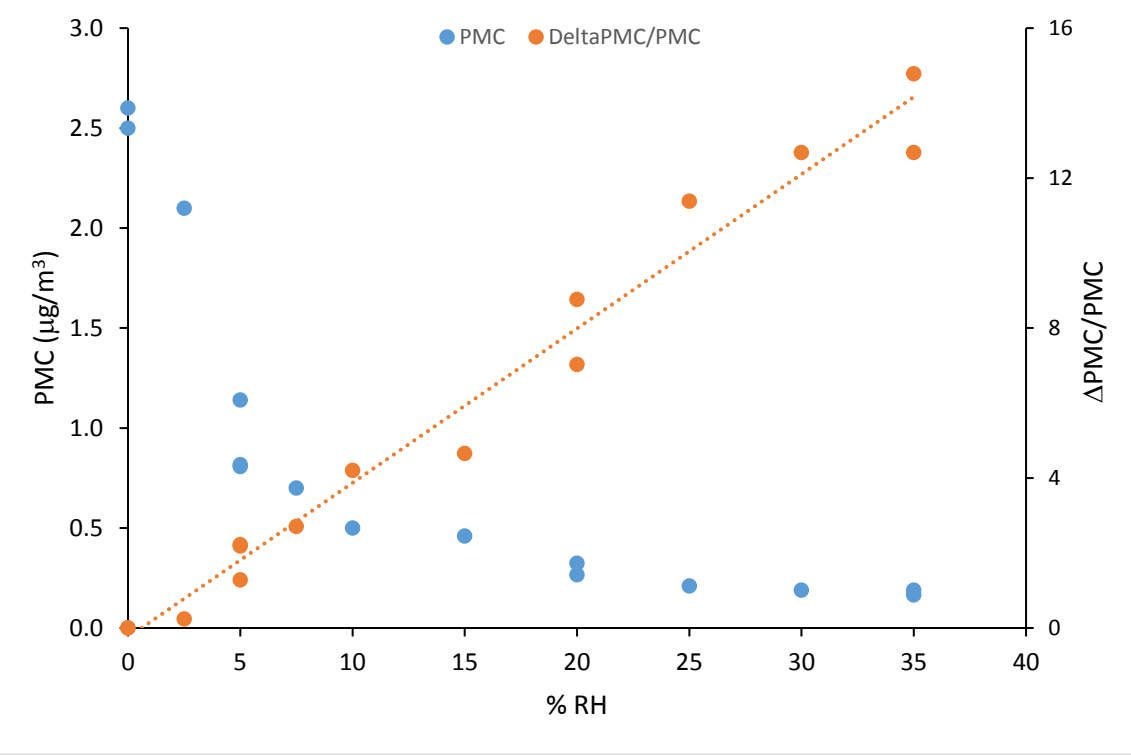

Figure 7. Water effect on the particle mass concentration. For this series of experiments, the concentration ratios were 20 ppb, 20 ppb and 40 ppb for styrene, SO_2 and ozone, respectively. The plotted PMC data plotted for each experiment are those obtained at 40' reaction time.

The rates of the sCI reactions towards SO_2 and H_2O depend on their concentrations and their kinetic rate constants, k_{SO2} and k_{H2O}. Since both [H_2O] and [SO_2] are known (and essentially constant during the experiments), experimental data of the products of these reaction can provide the ratio of theses competitive reactions (k_{H2O}/k_{SO2}). Thus, considering the dry experiments (0% RH) as reference, we can assume that for the experiments carried out in the presence of water the decrease in mass concentration, $\Delta_{PMC} = PMC_{RH=0} - PMC$, is due exclusively to the reaction of the sCI with water molecules. Thus, the ratio (k_{H2O} [H_2O])/(k_{SO2}[SO_2]) can be obtained as the ratio Δ_{PMC} /PMC (Díaz-de-Mera et al., 2017), assuming that the reaction of sCI with SO_2 is the sole source of SOA. Then, the linear fit of the plot (Δ_{PMC} /PMC) versus [H_2O], Figure 7, provides the (k_{H2O}/(k_{SO2}[SO_2])) ratio from the slope, and then the ratio between the rate constants, k_{H2O}/k_{SO2}= $(2.8\pm0.7)\times10^{-5}$ (the SO_2 concentration is known, 20 ppb=$4.9x10^{11}$ molecule cm^{-3}, errors are $2\sigma\pm20\%$).

This result is similar to other reported values for different CI (Berndt et al., 2014a, Díaz-de-Mera et al., 2017) and may be used to assess the effects of SO_2 and water vapour in the formation of SOA under different atmospheric conditions.

4. Conclusions.

Previous studies have shown the outstanding potential of SOA formation due to the emissions of aromatic compounds to the atmosphere. Among them, styrene is one of the aromatics with the highest contribution to SOA. Although the formation of new particles from the ozonolysis of styrene has been reported from laboratory experiments, this reaction can't justify such high capacity to form new particles since it would require high concentrations of reactants compared to those of real polluted atmospheres. Generally, atmospheric models based on laboratory chamber studies predict far less SOA than is observed in field studies (Kroll and Seinfeld, 2008). This fact suggest that other yet unknown pathways may lead to the formation of new particles more effectively. In this sense, SO_2 may play a key role since, as found in this work, the ozonolysis of styrene in the presence of low concentrations of SO_2 readily produces new particles. The nucleation events occur at concentration around $(5.6\pm1.7)x10^8$ molecule cm^{-3}, that is, 3 orders of magnitude below that of the reaction in the absence of SO_2.

The particle mass concentration temporal profiles correlate with the reacted styrene showing that the ozonolysis of styrene is the rate limiting step in the formation of new particles. The fractional yields for different initial concentrations of reactants have been obtained based on the amount of reacted styrene. They are independent on the concentrations of styrene or ozone but increase from nearly zero in the absence of SO_2 to approximately 2 when SO_2 is in excess.

The experimental temporal decays of SO_2 show that it reacts with the products of the ozonolysis of styrene. From the simulated profiles of reacted styrene, under low water concentration conditions (below 2 ppm) the yield for the consumption of SO_2 was $\eta = 0.51 \pm 0.13$. Thus, the formation of SO_3 from the reaction of styrene with the Criegee intermediates is expected to be responsible of the nucleation events through the formation of H_2SO_4. On the other hand, the presence of water in the reaction media competes with SO_2 and inhibits the formation of SOA. So the potential formation of SOA under atmospheric conditions depends on the concentration of SO_2 and relative humidity.

As shown in a previous work (le Person et al. 2006) OH-based and ozone-based lifetimes for styrene are 2.4h and 25h, respectively and so both reactions contribute as efficient gas-phase sinks. Although the initial OH reaction is faster than ozonolysis, it is not clear whether the OH reaction products contribute efficiently to the formation of aerosols, as it has been found for ozonolysis in the presence of SO_2. In this sense, the study of particles generation from OH reactions is also required to fully understand the contribution of styrene to the formation of secondary organic aerosols in urban areas.

Acknowledgments.

This work was supported by the Spanish Ministerio de Economía y Competitividad (project CGL2014-57087-R, FEDER co-funding) and by the University of Castilla La Mancha (projects GI20152950 and GI20163433).

References.

Anglada, J.M., González, J., Torrent-Sucarrat, M, 2011. Effects of the substituents on the reactivity of carbonyl oxides. A theoretical study on the reaction of substituted carbonyl oxides with water. Physical Chemistry Chemical Physics, 13, 13034–13045.

Atkinson, R. and Aschmann, S.M., 1988. Kinetics of the reactions of acenaphthene and acenaphthylene and structurally-related aromatic compounds with OH and NO_3 at 296±2K. International Journal of Chemical Kinetics, 20, 513-539.

ATSDR, 2017. https://www.atsdr.cdc.gov/toxprofiles/tp53-c3.pdf accesed June 2017.

Bates, J. T., Weber, R. J., Abrams, J., Verma, V., Fang, T., Klein, M., Strickland, M. J., Sarnat, S. E., Chang, H. H., Mulholland, J. A., Tolbert, P. E., Russell, A. G., 2015. Reactive oxygen species generation linked to sources of atmospheric particulate matter and cardiorespiratory effects. Environmental Science & Technology, 49(22), 13605-13612. DOI: 10.1021/acs.est.5b02967.

Berndt, T., Jokinen, T., Sipilä, M., Mauldin, R. L., Herrmann, H., Stratmann, F., Junninen, H., Kulmala, M., 2014a. H_2SO_4 formation from the gas-phase reaction of stabilized Criegee Intermediates with SO_2: Influence of water vapour content and temperature. Atmospheric Environment, 89, 603-612. DOI: org/10.1016/j.atmosenv.2014.02.062.

Berndt, T., Voigtländer, J., Stratmann, F., Junninen, H., Mauldin, R. L., Sipilä, M., Kulmala, M., Herrmann, H., 2014b. Competing atmospheric reactions of CH_2OO with SO_2 and water vapour. Physycal Chemistry Chemical Physics, 16, 19130-19136. DOI: 10.1039/C4CP02345E.

Cheung H.C., Chou C.C.K., Huang, W.R., Tsai, C.Y., 2013. Characterization of ultrafine particle number concentration and new particle formation in an urban environment of Taipei, Taiwan. Atmospheric Chemistry and Physics, 13(17), 8935–8946. DOI: 10.5194/acp-13-8935-2013.

Diaz-de-Mera, Y., Aranda, A., Bracco, L., Rodriguez, D., Rodriguez, A., 2017. Formation of secondary organic aerosols from the ozonolysis of dihydrofurans. Atmospheric Chemistry and Physics, 17(3), 2347-2357. DOI: org/10.5194/acp-17-2347-2017.

Duke, J.A., 1985, CRC handbook of medical herbs. Boca Raton, FL, CRC Press, p. 323.

EPA 2017, Initial list of hazardous air pollutants with modifications. https://www.epa.gov/haps/initial-list-hazardous-air-pollutants-modifications accesed June 2017.

Hu, N., Tan, J., Wang, X., Zhang, X., Yu, P., 2017. Volatile organic compound emissions from an engine fueled with an ethanol-biodiesel-diesel blend. Journal of the Energy Institute, 90, 101-109. DOI: org/10.1016/j.joei.2015.10.003.

Jayne, J. T., Pöschl, U., Chen, Y., Dai, D., Molina, L.T., Worsnop, D.R., Kolb, C.E., Molina, M. J., 1997. Pressure and temperature dependence of the gas-phase reaction of SO_3 with H_2O and the heterogeneous reaction of SO_3 with H_2O/H_2SO_4 surfaces. Journal of Physical Chemistry A, 101, 10000-10011. DOI: 10.1021/jp972549z.

Jiang, L., Xu, Y., Ding, A., 2010. Reaction of stabilized Criegee intermediates from ozonolysis of limonene with sulfur dioxide: ab initio and DFT study. J. Phys. Chem. A, 114, 12452-12461. DOI: 10.1021/jp107783z.

Kabir, E. and Kim, K. H., 2010. An on-line analysis of 7 odorous volatile organic compounds in the ambient air surrounding a large industrial complex. Atmospheric Environment, 44(29), 3492-3502. DOI: org/10.1016/j.atmosenv.2010.06.021.

Knighton, W. B., Herndon, S.C., Wood, E.C., Fortner, E.C.,Onasch, T. B., Wormhoudt, J., Kolb, C. E., Lee, B.H., Zavala, M., Molina, L., Jones, M., 2012. Detecting fugitive emissions of 1,3-butadiene and styrene from a petrochemical facility: An application of a mobile laboratory and a modified proton transfer reaction mass spectrometer. Industrial & Engineering Chemistry Research, 51 (39), 12706–12711. DOI: 10.1021/ie202794j.

Kos, G., Adechina, N., Kanthasamy, V., Ariya, P. A.,2014. Volatile organic compounds in Arctic snow: Concentrations and implications for atmospheric processes. RSC, Environmental Science: Processes & Impacts 16 (11), 2592-2603. DOI: 10.1039/C4EM00410H.

Kroll, J. H., Seinfeld, J. H., 2008. Chemistry of secondary organic aerosol: Formation and evolution of low-volatility organics in the atmosphere. Atmospheric Environment, 42(16), 3593-3624.

Kurtén, T., Lane, J. R., Jørgensen, S., Kjaergaard, H. G.,2011. A Computational Study of the Oxidation of SO_2 to SO_3 by Gas-Phase Organic Oxidants. J. Phys. Chem. A, 115 (31), 8669–8681. DOI: 10.1021/jp203907d.

Le Person, A., Eyglunent, G., Daele, V., Mellouki, A., Mu, Y. 2008. The near UV absorption cross-sections and the rate coefficients for the ozonolysis of a series of styrene-like compounds. Journal of Photochemistry and Photobiology A: Chemistry, 195(1), 54-63. DOI: org/10.1016/j.jphotochem.2007.09.006.

Li, L., Li, H., Zhang, X., Wang, L., Xu, L., Wang, X., ... & Cao, G. 2014. Pollution characteristics and health risk assessment of benzene homologues in ambient air in the northeastern urban area of Beijing, China. Journal of Environmental Sciences, *26*(1), 214-223. https://doi.org/10.1016/S1001-0742(13)60400-3.

Li, L., Ge, Y., Wang, M., Peng, Z., Song, Y., Zhang, L., Yuan, W., 2015. Exhaust and evaporative emissions from motorcycles fueled with ethanol gasoline blends. Science of the Total Environment, 502, 627-631. DOI: org/10.1016/j.scitotenv.2014.09.068.

Li, L., Tang, P., Nakao, S., Kacarab, M., Cocker III, D. R., 2016. Novel approach for evaluating secondary organic aerosol from aromatic hydrocarbons: Unified method for predicting aerosol composition and formation. Environmental Science & Technology, 50(12), 6249-6256. DOI: 10.1021/acs.est.5b05778.

Liu, T., Wang, X., Hu, Q., Deng, W., Zhang, Y., Ding, X., Fu, X., Bernard, F., Zhang, Z., Lü, S., He, Q., Bi, X., Chen, J., Sun, Y., Yu, J., Peng, P., Sheng, G., and Fu, J. 2016. Formation of secondary aerosols from gasoline vehicle exhaust when mixing with SO2, Atmos. Chem. Phys., 16, 675-689, doi:10.5194/acp-16-675-2016.

Lopes, M., Serrano, L., Ribeiro, I., Cascão, P., Pires, N., Rafael, S., Tarelho,L., Monteiro, A., Nunes, T., Evtyugina, M., Nielsen, O.J., Gameiro da Silva, M., Miranda, A.I., Borrego, C., 2014. Emissions characterization from EURO 5 diesel/biodiesel passenger car operating under the new European driving cycle. Atmospheric Environment, 84, 339-348. DOI: org/10.1016/j.atmosenv.2013.11.071.

Ma, Y., Porter, R.A., Chappell, D., Andrew, A.T., Russell, T., Marston, G., 2009. Mechanisms for the formation of organic acids in the gas-phase ozonolysis of 3-carene. Physical Chemistry Chemical Physics, 11, 4184–4197.

Mauldin, R. L., Berndt, T., Sipilä, M., Paasonen, P., Petäjä, T., Kim, S., Kurtén, T., Stratmann, F., Kerminen, V. M., Kulmala, M., 2012. A new atmospherically relevant oxidant of sulphur dioxide. Nature, 488, 193–196. DOI: 10.1038/nature11278.

Mejía, J. F., Morawska, L., and Mengersen, K., 2008. Spatial variation in particle number size distributions in a large metropolitan area, Atmos. Chem. Phys., 8, 1127-1138. Doi:10.5194/acp-8-1127-2008.

Na, K., Song, C., Cocker, D. R., 2006. Formation of secondary organic aerosol from the reaction of styrene with ozone in the presence and absence of ammonia and water. Atmospheric Environment, 40(10), 1889-1900. DOI: org/10.1016/j.atmosenv.2005.10.063.

Nel, A. 2005. Air pollution-related illness: effects of particles. Science, 308(5723), 804-806. DOI: 10.1126/science.1108752.

Newland, M. J., Rickard, A. R., Alam, M. S., Vereecken, L. Muñoz, A., Ródenas, M., Bloss, W.J., 2015. Kinetics of stabilised Criegee intermediates derived from alkene ozonolysis: reactions with SO_2, H_2O and decomposition under boundary layer conditions. Physical Chemistry Chemical Physics, 17, 4076-4088. DOI: 10.1039/C4CP04186K.

Ng, N. L., Kroll, J. H.; Chan, A. W. H., Chhabra, P. S., Flagan, R. C., Seinfeld, J. H., 2007. Secondary organic aerosol formation from mxylene, toluene, and benzene. Atmospheric Chemistry and Physics. 2007, 7 (14), 3909− 3922. DOI: 10.5194/acp-7-3909-2007.

Odum, J.R., Hoffman, T., Bowman, F., Collins, D., Flagan, R.C., Sienfeld, J.H., 1996. Gas/particle partitioning and secondary aerosol yields. Enviromental Science & Technology, 30, 2580-2585.

Sarigiannis, D.A., Karakitsios, S.P., Gotti, A., Liakos, I.L., Katsoyiannis, A., 2011. Exposure to major volatile organic compounds and carbonyls in European indoor environments and associated health risk. Environment International, 37, 743–765. DOI: org/10.1016/j.envint.2011.01.005.

Shimada, K., Kimura, E., Yasui, Y., Tanaka, H., Matsushita, S., Hagihara, H., Nagakura, M, Kawahisa, M., 1992. Styrene formation by the decomposition by Pichia carsonii of trans-cinnamic acid added to a ground fish product. Applied Environmental Microbiology, 58, 1577–1582.

Sun, J., Wu, F., Hu, B., Tang, G., Zhang, J., Wang, Y., 2016. VOC characteristics emissions and contributions to SOA formation during hazy episodes. Atmospheric Environment, 141, 560-570. DOI: org/10.1016/j.atmosenv.2016.06.060.

Taatjes C.A., Welz, O., Eskola, A.J., Savee, J.D., Scheer A.M., Shallcross, D.E., Rotavera, B., Lee, E.P., Dyke, J.M., Mok, D.K., Osborn, D.L., Percival, C.J., 2013. Direct measurements of conformer-dependent reactivity of the Criegee intermediate CH3CHOO. Science. 12, 340(6129), 177-180. DOI: 10.1126/science.1234689.

Tuazon, E. C., Arey, J., Atkinson, R., Aschmann, S. M., 1993. Gas-phase reactions of 2-vinylpyridine and styrene with hydroxyl and NO_3 radicals and ozone. Environmental Science & Technology, 27(9), 1832-1841. DOI: 10.1021/es00046a011.

Vereecken, L. and Francisco, J. S., 2012. Theoretical studies of atmospheric reaction mechanisms in the troposphere. Chemical Society Reviews, 41(19), 6259-6293. DOI: 10.1039/C2CS35070J.

Wang, H., Ji, Y., Gao, Y., Li, G., An, T. 2015. Theoretical model on the formation possibility of secondary organic aerosol from OH initialed oxidation reaction of styrene in the presence of O_2/NO. Atmospheric Environment, 101, 1-9. DOI: org/10.1016/j.atmosenv.2014.10.042.

Welz, O., Savee, J. D., Osborn, D. L., Vasu, S. S., Percival, C. J, Shallcross, D., Taatjes, C., 2012. Reaction of CH_2I with O_2 forms Criegee Intermediate: Direct Measurements of CH_2OO Kinetics. Science, 335, 204-207. DOI: 10.1126/science.1213229.

Xu, J., Szyszkowicz, M., Jovic, B., Cakmak, S., Austin, C. C., Zhu, J., 2016. Estimation of indoor and outdoor ratios of selected volatile organic compounds in Canada. Atmospheric Environment, 141, 523-531. DOI: org/10.1016/j.atmosenv.2016.07.031.

Zhang, Z., Wang, H., Chen, D., Li, Q., Thai, P., Gong, D., Li, Y., Zhang, C., Gu, Y., Zhou, L., Morawska, L., Wang, B., 2017. Emission characteristics of volatile organic compounds and their secondary organic aerosol formation potentials from a petroleum refinery in Pearl River Delta, China. Science of the Total Environment, 584-585, 1162-1174. DOI: 10.1016/j.scitotenv.2017.01.179.